Solid State Sciences 12 (2010) 199–203

Contents lists available at ScienceDirect

Solid State Sciences

journal homepage: www.elsevier.com/locate/ssscie

# Impact of the exchange-correlation functional on the structure of glassy $GeSe_2$

Carlo Massobrio [a,*], Matthieu Micoulaut [b], Philip S. Salmon [c]

[a] Institut de Physique et de Chimie des Matériaux de Strasbourg, 23 rue du Loess, BP 43, F-67034 Strasbourg Cedex 2, France
[b] Laboratoire de Physique Théorique de la Matière Condensée, Université Pierre et Marie Curie, 4 Place Jussieu, F-75252 Paris Cedex 05, France
[c] Department of Physics, University of Bath, Bath BA2 7AY, UK

ARTICLE INFO

*Article history:*
Received 9 November 2009
Received in revised form
23 November 2009
Accepted 23 November 2009
Available online 29 November 2009

*Keywords:*
Disordered materials
Density functional theory
Molecular dynamics

ABSTRACT

The structural properties of glassy $GeSe_2$ were studied by using first-principles molecular dynamics with the Becke, Lee, Yang and Parr (BLYP) expression for the exchange-correlation energy within density functional theory. A comparison is made with the results previously obtained for this material by using first-principles molecular dynamics with the Perdew and Wang (PW) exchange-correlation functional. Overall, the structures of the BLYP-$GeSe_2$ and PW-$GeSe_2$ networks are quite similar, the BLYP approach favoring a larger number of Ge–Ge homopolar bonds, in better agreement with the experimental results. The BLYP network does, however, feature a smaller fraction of corner-sharing motifs by comparison with the PW network but the fraction of edge-sharing motifs is the same for both structures, at least within the confines of an approach based on a single temporal trajectory. Further studies are required to determine whether agreement between the BLYP structure and experiment can be improved by taking the average over a larger number of temporal trajectories or whether additional developments are required for the exchange-correlation part of the energy functional.



## 1. Introduction

One of the crucial ingredients for ensuring that network-forming disordered materials can be realistically modelled is an explicit account of the electronic structure [1,2]. In most cases, a correct description of the connections between various structural units (including edge-sharing *vs* corner-sharing configurations, homopolar bonds and rings of motifs) can only be obtained within the framework of a first-principles approach, in which no hypotheses are made about the charge distribution and the electron density has a non-trivial spatial extent. The valence electrons can be thought of as being located *around* the atomic sites and *in between* them, the correct proportion of these two parts being highly sensitive to the specific treatment of the electronic structure. In the case of chalcogenide materials, special attention has been devoted to the spatial distribution of the electronic charge in liquid $GeSe_2$ ($l$-$GeSe_2$) owing, in part, to the similar electronegativities of the different atomic species [1,3,4].

For $l$-$GeSe_2$, a detailed comparison has been made between the pair correlation functions, partial structure factors and coordination numbers obtained by using the first-principles methodology with three different approximations for the exchange-correlation (XC) parts of the Kohn–Sham Hamiltonian in density functional theory (DFT). Specifically, the local density approximation (LDA), the generalized gradient approximation (GGA) due to Perdew and Wang (PW) and the generalized gradient approximation due to Becke, Perdew, Yang and Parr (BLYP) were investigated [4]. It was found that the atomic structure obtained by using the LDA was affected by an excessive amount of chemical disorder (configurations other than Ge coordinated to 4 Se atoms and Se coordinated to 2 Ge atoms) and homopolar bonds. The PW approach improved upon the LDA bringing theory into an overall satisfactory agreement with experiment. This improvement was due to a better account of the system ionicity which manifests itself through a larger depletion of the valence electron charge density at the Ge sites and a larger accumulation of this density around the Se sites [1]. Residual shortcomings of the PW approach were attributed to an insufficiently accurate description of Ge–Ge correlations. The shape of the calculated Ge–Ge pair correlation function $g_{GeGe}(r)$ was much less structured than its experimental counterpart and the mean first-neighbor Ge–Ge distance was excessively long being 15% larger than the experimental value [3]. These observations prompted the use of a GGA functional which enhances a *localized* distribution of the valence electrons at the expense of a *delocalized* one, the latter being intrinsic to schemes inspired by a uniform electron gas model as in the PW approach. Application of the BLYP scheme to $l$-$GeSe_2$ led to a shape for the Ge–Ge pair correlation function that is closer to the experimental one and the level of

* Corresponding author.
*E-mail address:* carlo.massobrio@ipcms.u-strasbg.fr (C. Massobrio).

1293-2558/$ – see front matter © 2009 Elsevier Masson SAS. All rights reserved.
doi:10.1016/j.solidstatesciences.2009.11.016

structural organization (the number of non-defected $GeSe_4$ tetrahedra) was enhanced. It thus appears that use of the BLYP scheme improves our DFT model of *l*-$GeSe_2$ by granting it a more quantitative character [4].

The structure of glassy $GeSe_2$ (*g*-$GeSe_2$) has been the subject of a large number of different experimental and computer simulation studies [2,5–16]. The PW approach has led to a picture for this network-forming material that is broadly in line with neutron diffraction data [17]. However, as in the case of *l*-$GeSe_2$, $g_{GeGe}(r)$ is much less structured around the main peak and the concentration of Ge–Ge homopolar bonds is lower than found by experiment. It is therefore of interest to carry out a new set of calculations aimed at describing the structural properties of *g*-$GeSe_2$ by using the BLYP approach. This will allow for an instructive comparison to be made between the PW and BLYP results and it is this task that is accomplished in the present paper.

The manuscript is organized as follows. In Section. 2 we describe the methodology used to generate a structure for *g*-$GeSe_2$ using the BLYP XC functional. The results are collected in two sections, one devoted to the real space properties (Section. 3) and the other to the reciprocal space properties (Section. 4). Concluding remarks are given in Section. 5.

## 2. Theoretical model

The simulations were performed at constant volume on a system consisting of 120 atoms (40 Ge and 80 Se). A periodically repeated cubic cell of side length 15.16 Å was used, corresponding to a number density of 0.034 $Å^{-3}$ at a temperature $T = 300$ K, slightly larger than the value quoted in the corresponding experimental work (0.0334 $Å^{-3}$) [18]. The electronic structure was described within density functional theory and evolved self-consistently during the motion [19,20]. Valence electrons were treated explicitly, in conjunction with normconserving pseudopotentials to account for core–valence interactions. The wave functions were expanded at the $\Gamma$ point of the supercell and the energy cutoff was set at $E_c = 20$ Ry. We refer to our previous study of liquid $GeSe_2$ for many of the technical ingredients of the simulations, such as the energy cutoff for the expansion of the wave functions on a plane-wave basis set, the value of the fictitious electron mass and the detail of test calculations carried out on a GeSe dimer [3].

Concerning the choice of XC functional, the PW scheme was adopted in the past [1,3,17]. This goes beyond the local density approximation (LDA) by using an analytic representation for the correlation energy $\varepsilon_c(\rho)$ of a uniform electron gas. This representation allows for a variation of $\varepsilon_c(\rho)$ with the charge density $\rho$ and spin polarization [22]. By comparison with the LDA method, the PW scheme leads to a substantial improvement in description of both the short and intermediate range order in *l*-$GeSe_2$. However, there were still differences between theory and experiment which could be rationalized in terms of an insufficiently accurate description of Ge–Ge correlations, with excessively long Ge–Ge bond lengths that are characteristic of metallic liquid Ge [23–26].

In the search for a GGA recipe correcting these defects, we resort in this work to the generalized gradient approximation after Becke (B) for the exchange energy and Lee, Yang and Parr (LYP) for the correlation energy [27,28]. Our choice is motivated by the fact that no explicit reference to a uniform electron gas is made in the derivation of the LYP correlation energy [28,29]. This scheme enhances the localized behavior of the electron density at the expense of electronic delocalization effects that favor a metallic character. These effects are built into GGA recipes having the uniform electron gas as a reference system, as in the case of the PW scheme. We refer to our recent work on a comparison between the PW and BLYP structures of *l*-$GeSe_2$ for a more detailed rationale about the reasons underlying our choice of the BLYP XC functional [4]. It has to be underlined that the PW and BLYP schemes differ only in the treatment of the correlation energy since the exchange energy, due to Becke, is the same for both approaches [27].

In the following, the comparison between the PW and BLYP structures makes use of the PW data of Ref. [21]. From the temporal trajectory in the liquid state used to obtain the results presented in Ref. [21], we have selected one configuration as the initial one for the BLYP calculations. The system was left to evolve at a temperature of 900 K for 50 ps by using a Nosé–Hoover thermostat [30,31]. The system was then annealed at $T = 600$ K for 20 ps and at $T = 300$ K for a final trajectory of 10 ps during which statistical averages were collected. The interval of 50 ps at $T = 900$ K allowed for significant atomic diffusion and ensured that memory of the initial configuration was lost. This quenching schedule does not differ significantly from the one adopted in Ref. [21] where configurations for the glass at $T = 300$ K were collected by cooling the system from the liquid state at 1100 K down to 600 K in 22 ps (10 ps at 1100 K, 7 ps at 900 K and 5 ps at 600 K) and by annealing for 22 ps at $T = 300$ K.

Care must be exercised when comparing the averages obtained from only one temporal trajectory. In Ref. [17], it was pointed out that substantial statistical errors affect the overall averages obtained for the structural properties of glassy systems. This conclusion was drawn by observing the behavior of representative quantities (pair correlation functions, coordination numbers, number of homopolar bonds) calculated for several independent trajectories starting from uncorrelated liquid configurations. We will use these results to guide us in assessing the significance of the differences found between the structural quantities calculated by using the PW and BLYP approaches. Accordingly, discrepancies between the structures that were obtained will not be highlighted unless they lie outside the error bars previously established in the case of glassy $GeSe_2$ (PW calculations) for a set of six independent trajectories [17].

## 3. Real space properties

In Fig. 1 we display the calculated and experimental partial pair correlation functions (PCFs) calculated by using the PW (Ref. [21]) and BLYP (present work) approaches. The peak positions and coordination numbers $n_{\alpha\beta}$ extracted from the PCFs are listed in Table 1, where they are compared with the experimental data taken from Table 2 of Ref. [14]. In the case of $g_{SeSe}(r)$, there are no substantial differences between the PW and BLYP results. The PW and BLYP calculations both give a higher intensity for the first peak in $g_{SeSe}(r)$, resulting in a moderate overestimate of the corresponding coordination number $n_{SeSe}$ for homopolar bonds, namely $n_{SeSe}^{expt} = 0.2$, $n_{SeSe}^{PW} = 0.24$, $n_{SeSe}^{BLYP} = 0.30$.

As seen in Fig. 1, $g_{GeSe}^{BLYP}(r)$ and $g_{GeSe}^{PW}(r)$ are both in good agreement with experiment in terms of the position and width of the main peak. On the experimental side, the intensity of this peak is slightly higher and the decay to zero with increasing distance $r$ is more abrupt than for both $g_{GeSe}^{BLYP}(r)$ and $g_{GeSe}^{PW}(r)$. The finite values of $g_{GeSe}^{PW}(r)$ in between 2.5 Å and 3 Å contribute to a larger coordination number $n_{GeSe}$ as obtained by integrating over the first peak in the Ge–Se PCF up to the first minimum, namely $n_{GeSe}^{PW} = 3.92$ compared to $n_{GeSe}^{exp} = 3.7$. The BLYP XC functional has the effect of inducing a more rapid decay to zero of the main peak, resulting in a better value for the coordination number, $n_{GeSe}^{BLYP} = 3.58$.

The comparison between $g_{GeGe}^{PW}(r)$, $g_{GeGe}^{BLYP}(r)$ and $g_{GeGe}^{exp}(r)$ in Fig. 1 shows three distinct features in the region $2 \lesssim r(Å) \lesssim 4$. The first and third features show up as distinct peaks, while the second feature is discernible as a shoulder in both $g_{GeGe}^{exp}(r)$ and $g_{GeGe}^{PW}(r)$, becoming a peak in $g_{GeGe}^{BLYP}(r)$. With increasing $r$, these peaks and/or

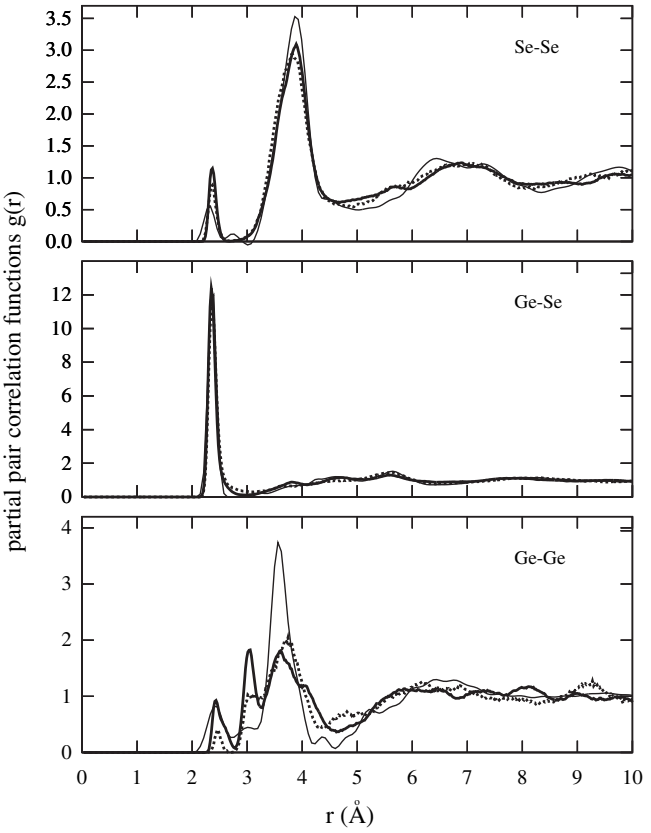


**Fig. 1.** The partial pair correlation functions (PCFs) for glassy $GeSe_2$. The experimental results of Ref. [13] (thin solid curves) are compared with the PW results of Ref. [21] (dotted curves) and with the present BLYP results (thick solid curves).

**Table 1**
The first peak (FP), second peak (SP) and third peak (TP) positions in the experimental (Ref. [14]) and theoretical $g_{\alpha\beta}(r)$ functions where PW stands for the results of Ref. [21] and BLYP for the present results. $n_{\alpha\beta}$, $n'_{\alpha\beta}$ and $n''_{\alpha\beta}$ are the coordination numbers corresponding to the FP, SP and TP, respectively, and refer to the number of atoms of type $\beta$ surrounding an atom of type $\alpha$. IR represents the integration range for each coordination number. In our calculations the IRs are taken as the intervals between the two minima preceding and following a maximum. Note that the models gave no signature of a second peak in $g_{SeSe}(r)$ so, for clarity of presentation, the peak position, integration range and coordination number obtained from the second peak in $g^{PW}_{SeSe}(r)$ and $g^{BLYP}_{SeSe}(r)$ are compared to the corresponding values for the third peak in the experimental Se–Se function.

| $g_{\alpha\beta}(r)$ | FP (Å) | $n_{\alpha\beta}$ | IR [FP](Å) | SP (Å) | $n'_{\alpha\beta}$ | IR [SP](Å) |
|---|---|---|---|---|---|---|
| $g^{exp}_{GeGe}(r)$ | 2.42 | 0.25 | 0–2.73 | 3.02 | 0.34 | 2.73–3.19 |
| $g^{PW}_{GeGe}(r)$ | 2.45 | 0.05 | 0–2.70 | 3.11 | 0.32 | 2.70–3.14 |
| $g^{BLYP}_{GeGe}(r)$ | 2.43 | 0.20 | 0–2.78 | 3.11 | 0.69 | 2.78–3.27 |
| $g^{exp}_{GeSe}(r)$ | 2.36 | 3.7 | 2.09–2.61 | | | |
| $g^{PW}_{GeSe}(r)$ | 2.37 | 3.92 | 2.11–3.12 | | | |
| $g^{BLYP}_{GeSe}(r)$ | 2.35 | 3.58 | 2.07–3.04 | | | |
| $g^{exp}_{SeSe}(r)$ | 2.32 | 0.20 | 0–2.55 | 2.74 | 0.06 | 2.55–3.09 |
| $g^{PW}_{SeSe}(r)$ | 2.37 | 0.24 | 0–2.70 | | | |
| $g^{BLYP}_{SeSe}(r)$ | 2.37 | 0.30 | 0–2.65 | | | |
| | TP (Å) | | $n''_{\alpha\beta}$ | | IR [TP](Å) | |
| $g^{exp}_{GeGe}(r)$ | 3.57 | | 3.2 | | 3.19–4.23 | |
| $g^{PW}_{GeGe}(r)$ | 3.74 | | 3.02 | | 3.14–4.34 | |
| $g^{BLYP}_{GeGe}(r)$ | 3.61 | | 3.15 | | 3.27–4.62 | |
| $g^{exp}_{SeSe}(r)$ | 3.89 | | 9.3 | | 3.09–4.39 | |
| $g^{PW}_{SeSe}(r)$ | 3.81 | | 9.85 | | 2.70–4.62 | |
| $g^{BLYP}_{SeSe}(r)$ | 3.89 | | 9.90 | | 2.67–4.64 | |

**Table 2**
The average number of dimers, trimers, tetramers and pentamers for the Ge and Se atomic species. The numbers in parentheses are the results obtained in Ref. [21] by using the Perdew-Wang (PW) exchange-correlation functional. We also compare the calculated and experimental values (in percent) for the fraction of Ge atoms in Ge–Ge homopolar bonds, $N_{Ge-Ge}$, the fraction of Se atoms in Se–Se homopolar bonds, $N_{Se-Se}$, the fraction of Ge atoms forming edge-sharing connections, $N_{Ge}(ES)$, and the fraction of Ge atoms forming corner-sharing connections, $N_{Ge}(CS)$. It should be noted that the values of $N_{Ge}(ES)$ and $N_{Ge}(CS)$ differ from those given in Ref. [21] since a different approach has been used to extract these numbers from the atomic configurations (see the text).

| | Dimers | Trimers | Tetramers | Pentamers |
|---|---|---|---|---|
| Ge | 4(1) | – | – | – |
| Se | 4(8) | 2(1) | –(–) | 1(–) |
| | $N_{Ge-Ge}$ | $N_{Se-Se}$ | $N_{Ge}(ES)$ | $N_{Ge}(CS)$ |
| PW | 5 | 24 | 58 | 37 |
| BLYP | 20 | 30 | 58 | 22 |
| Experiment: Ref. [14] | 25 | 20 | 34 | 41 |

shoulders can be identified with homopolar Ge–Ge bonds, Ge atoms involved in edge-sharing connections, and Ge atoms involved in corner-sharing connections, respectively. Interestingly, $g^{BLYP}_{GeGe}(r)$ has a more pronounced minimum than $g^{PW}_{GeGe}(r)$ at $r \gtrsim 4$ Å, consistent with the case of *l*-$GeSe_2$ [4]. In the BLYP model, the intensity of the first peak is very close to the experimental one, improving upon the PW results. Accordingly, the fraction of Ge atoms involved in homopolar bonds (8/40 = 20%) is in reasonable accord with the experimental value of 25% [13,14].

In the experimental work of Ref. [14], the coordination number obtained by integrating over the shoulder at ≈3 Å in the Ge–Ge PCF was used to estimate the fraction of Ge atoms in edge-sharing connections ($N_{Ge}(ES) = 0.34$). By following the same procedure, a value $N_{Ge}(ES) = 0.32$ was reported in Table 2 of Ref. [21] for the PW network and a much larger value of $N_{Ge}(ES) = 0.69$ is obtained for the present BLYP structure. The latter value is in line with the presence of a sharp second peak in $g^{BLYP}_{GeGe}(r)$ (see Fig. 1). An alternative method to obtain the fraction of Ge atoms involved in edge-sharing connections is to enumerate the number of Ge atoms participating in four-fold rings [17]. This choice has the advantage of including all edge-sharing connections, without excluding those in which the Ge atoms are separated by a distance larger than the second minimum in $g_{GeGe}(r)$. This method was adopted to compile the $N_{Ge}(ES)$ values given in Table 2 for the PW and BLYP structures. Accordingly, the PW results for $N_{Ge}(ES)$ listed in this table supersede those given in Table 2 of Ref. [21]. The PW and BLYP calculations give identical values of $N_{Ge}(ES) = 0.58$, overestimating the experimental value of $N_{Ge}(ES) = 0.34$.

In Table 2 we list the fraction (in percent) of Ge or Se atoms involved in homopolar bonds, $N_{Ge-Ge}$ or $N_{Se-Se}$, along with the fraction (in percent) of Ge atoms forming corner-sharing [$N_{Ge}(CS)$] or edge-sharing [$N_{Ge}(ES)$] connections. To obtain $N_{Ge}(CS)$ we follow the procedure used in Ref. [14], where $N_{Ge}(CS) = 1 - N_{Ge}(ES) - N_{Ge-Ge}$, which holds in the absence of extended chains of Ge atoms either in edge-sharing configurations or in homopolar bonds. It appears that the BLYP scheme improves upon the PW scheme in predicting the number of Ge–Ge homopolar bonds, but a disagreement with experiment persists for the value of $N_{Ge}(ES)$. As a consequence, the value of $N_{Ge}(CS)$ is smaller for BLYP (22%) compared to PW (37%). Overall, the calculations appear to favor edge-sharing configurations at the expense of corner-sharing ones, the latter being more numerous in the experimental data of Ref. [14].

Information on the short range structure of *g*-$GeSe_2$ is given in Table 3. We define $n_\alpha(l)$ as the average number of atoms of species $\alpha$ that are *l*–fold coordinated, where $\alpha$ denotes a Ge or Se atom. The two sets of data for the BLYP and PW models appear to be quite

**Table 3**
The average number $n_\alpha(l)$ (bold font, expressed as a percentage) of atoms of species $\alpha$ ($\alpha$ = Ge, Se) that are $l$–fold coordinated at a distance of 2.7 Å. For each value of $n_\alpha(l)$ we give the identity and the number of Ge and Se neighbors. For instance, $GeSe_3$ in the column labeled $l = 4$ means a fourfold coordinated Ge atom with one Ge and three Se atom nearest-neighbors whereas $Se_4$ means a fourfold coordinated Ge atom with four Se atom nearest-neighbors. For comparison, the results are also given (in parentheses) from Ref. [21] where the structure was calculated by using the Perdew–Wang (PW) exchange-correlation functional.

| | | | | | |
|---|---|---|---|---|---|
| **Ge** | | $l = 1$ | **1.1(5.0)** | $l = 2$ | **10.8(11.1)** |
| | | Se | 1.1 (5.0) | GeSe | –(–) |
| | | | | $Se_2$ | 10.8 (11.1) |
| $l = 3$ | **9.9(5.9)** | $l = 4$ | **78.1 (75.6)** | $l = 5$ | –(**1.8**) |
| $GeSe_2$ | 2.6(–) | $GeSe_3$ | 15.6(5.0) | $Ge_2Se_3$ | –(–) |
| $Se_3$ | 7.3(5.9) | $Se_4$ | 62.5(70.6) | $GeSe_4$ | –(–) |
| | | | | $Se_5$ | –(1.8) |
| **Se** | | $l = 1$ | **1.1(2.3)** | $l = 2$ | **94.6(94.6)** |
| | | Se | –(–) | $Se_2$ | 6.2(1.2) |
| | | Ge | 1.1(2.3) | SeGe | 17.5(22.4) |
| | | | | $Ge_2$ | 71.0(71.0) |
| | | $l = 3$ | **4.3(3.0)** | | |
| | | $Ge_3$ | 4.3(3.0) | | |

similar. However, the increase in number of Ge–Ge homopolar bonds for the BLYP structure is reflected by a larger percentage of Ge atoms connected to 1 Ge atom and 2 Se atoms ($GeSe_2$ units) or to 1 Ge and 3 Se atoms ($GeSe_3$ units). Se atoms are organized in chains forming dimers, trimers and one pentamer. The number of Ge dimers (4 for the BLYP model against 1 for the PW model) is a mere consequence of the larger number of Ge–Ge homopolar bonds.

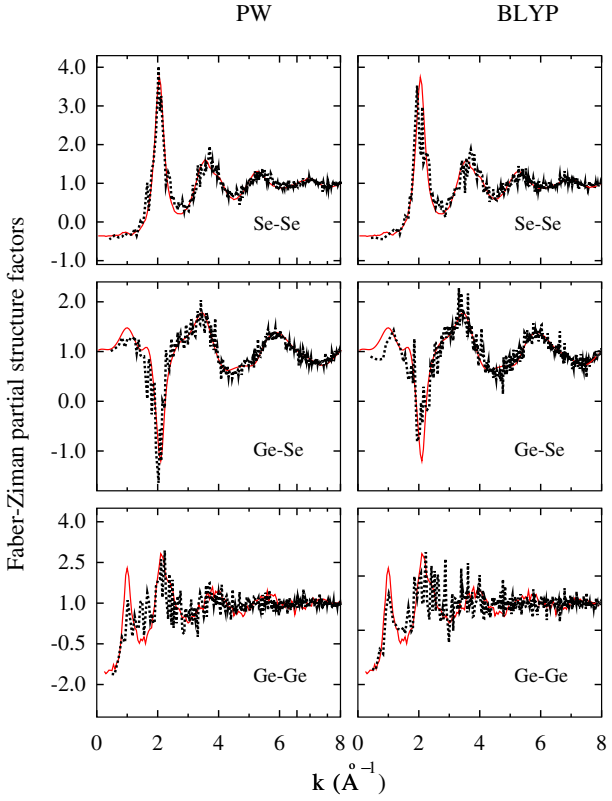


**Fig. 2.** The Faber–Ziman partial structure factors for glassy $GeSe_2$. The experimental results of Ref. [13] (thin solid curves (red in color on line)) are compared with the PW results of Ref. [21] (dotted curves, left panels) and with the present BLYP results (dotted curves, right panels).

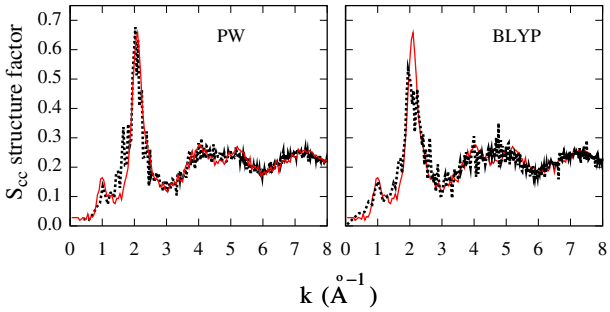


**Fig. 3.** The Bhatia–Thornton concentration–concentration partial structure factor $S_{CC}(k)$ for glassy $GeSe_2$. The experimental results of Ref. [13] (thin solid curves (red in color on line)) are compared with the PW results of Ref. [21] (dotted curve, left panel) and with the present BLYP results (dotted curve, right panel).

## 4. Reciprocal space properties

The Faber–Ziman partial structure factors $S_{SeSe}(k)$, $S_{GeSe}(k)$ and $S_{GeGe}(k)$ are shown in Fig. 2. In the case of $S_{SeSe}(k)$ and $S_{GeSe}(k)$, the two levels of theory (PW and BLYP) have comparable performances, notwithstanding the spurious spikes due to statistical noise. The comparison is less satisfactory for $S_{GeGe}(k)$. As discussed in Ref. [17], the theoretical $S^{PW}_{GeGe}(k)$ function is less structured than the experimental one. In particular, $S^{PW}_{GeGe}(k)$ does not show a pronounced minimum between the first two peaks and the height of the FSDP is lower. These deficiencies are partially cured by the BLYP approach. In $S^{BLYP}_{GeGe}(k)$, the FSDP has a more regular profile and it is followed by a clear first minimum. This improvement coincides with a deeper minimum in $g^{BLYP}_{GeGe}(r)$ at $r \gtrsim 4$ Å.

To examine the chemical ordering in $g$-$GeSe_2$, it is of interest to calculate the Bhatia–Thornton [32–34] concentration–concentration partial structure factor $S_{CC}(k)$, defined as

$$S_{CC}(k) = c_{Ge}c_{Se} + \{c_{Ge}c_{Se}[(S_{GeGe}(k) - S_{GeSe}(k)) + (S_{SeSe}(k) - S_{GeSe}(k))]\}, \quad (1)$$

where $S_{SeSe}(k)$, $S_{GeSe}(k)$ and $S_{GeGe}(k)$ are the Faber–Ziman partial structure factors while $c_{Ge}$ and $c_{Se}$ are the atomic fraction of Ge and Se atoms, respectively. Both $S^{PW}_{CC}(k)$ and $S^{BLYP}_{CC}(k)$ agree well with their experimental counterpart (see Fig. 3), although the calculated principal peak has a smaller intensity in the case of $S^{BLYP}_{CC}(k)$. We notice that an FSDP is clearly discernible at the correct location $k_{FSDP} = 1$ Å$^{-1}$. The presence of an FSDP in $S_{CC}(k)$ is consistent with the previously identified relationship between the appearance of this feature and a small departure from chemical order [35]. Indeed, the intensity found for the FSDP in $S_{CC}(k)$ for $g$-$GeSe_2$ is comparable to that for the $g$-$SiSe_2$ system where there is also a moderate departure from chemical order [35].

Taken altogether, the results for the partial structure factors indicate that the intermediate range order is less sensitive to the change in the exchange-correlation functional than the short range order, at least in so far as the different percentages of corner-sharing and edge-sharing connections inherent in the PW and BLYP structures have little effect on the intensity of the FSDP in either $S_{GeGe}(k)$ or $S_{CC}(k)$. However, further trajectories need to be taken for the BLYP approach to improve the statistical precision and hence shed more light on this issue.

## 5. Conclusions

We have compared the structural properties of glassy $GeSe_2$ obtained via first-principles molecular dynamics using two distinct DFT Kohn–Sham expressions for the total energy, differing in the

form taken by the exchange-correlation functional. The first, due to Perdew and Wang (PW), is based on an extension of the uniform electron gas approximation. The second, due to Lee, Yang and Parr for the correlation part and to Becke for the exchange part (BLYP), makes no reference to a uniform electron gas and it is expected to enhance charge localisation properties, partially correcting for the residual metallic-like behavior of the PW results. To this end, we have compared the PW results previously obtained with the new set of data obtained within the BLYP framework. A similar analysis has recently been published for the case of liquid $GeSe_2$ [4]. The most striking result from the BLYP set of calculations is the increased number of Ge–Ge homopolar bonds, in much better agreement with the experimental results.

Residual differences with experiment remain at the level of the $g_{GeGe}(r)$ pair correlation function. As a main consequence, the fraction of Ge atoms in edge-sharing connections is overestimated at 58% for both the PW and BLYP structures compared with 34% for experiment. However, it should be recalled that an extended calculation of the structural properties of glassy $GeSe_2$ within the PW scheme resulted in a smaller fraction of Ge atoms in edge-sharing connections, namely $45 \pm 4\%$ [17]. It remains to be understood whether the results from the BLYP model can be improved by making more extensive calculations (e.g. by using longer runs and/or larger simulation boxes) or by devising further refinements to the exchange-correlation part of the DFT Kohn–Sham energy functional.

## Acknowledgement

The calculations were performed on the computers of the CINES national computer center (Montpellier, France).

## References

[1] C. Massobrio, A. Pasquarello, R. Car, J. Am. Chem. Soc. 121 (1999) 2943.
[2] M. Cobb, D.A. Drabold, R.L. Cappelletti, Phys. Rev. B 54 (1996) 12162.
[3] C. Massobrio, A. Pasquarello, R. Car, Phys. Rev. B 64 (2001) 144205.
[4] M. Micoulaut, R. Vuilleumier, C. Massobrio, Phys. Rev. B 79 (2009) 214205.
[5] P. Tronc, M. Bensoussan, A. Brenac, C. Sebenne, Phys. Rev. B 8 (1973) 5947.
[6] W.J. Bresser, P. Boolchand, P. Suranyi, J.P. de Neufville, Phys. Rev. Lett. 46 (1981) 1689.
[7] P. Boolchand, J. Grothaus, W.J. Bresser, P. Suranyi, Phys. Rev. B 25 (1982) 2975.
[8] S. Sugai, Phys. Rev. B 35 (1987) 1345.
[9] For early studies of disordered $GeSe_2$ systems based on the use of effective potentials see: P. Vashishta, R.K. Kalia, G.A. Antonio, I. Ebbsjö, Phys. Rev. Lett. 62 (1989) 1651;
P. Vashishta, R.K. Kalia, I. Ebbsjö, Phys. Rev. B 39 (1989) 6034;
H. Iyetomi, P. Vashishta, R.K. Kalia, Phys. Rev. B 43 (1991) 1726.
[10] A. Fischer-Colbrie, P.H. Fuoss, J. Non-Cryst. Solids 126 (1990) 1.
[11] For the application to amorphous $GeSe_2$ of a non-self-consistent electronic structure scheme based on the local density approximation and the use of a minimal basis set see: X. Zhang, D.A. Drabold, Phys. Rev. B 62 (2000) 15695;
M. Durandurdu, D.A. Drabold, Phys. Rev. B 65 (2002) 104208;
D.N. Tafen, D.A. Drabold, Phys. Rev. B 68 (2003) 165208;
P. Biswas, D.N. Tafen, D.A. Drabold, Phys. Rev. B 71 (2005) 054204;
D.N. Tafen, D.A. Drabold, Phys. Rev. B 71 (2005) 054206.
[12] P. Boolchand, W.J. Bresser, Philos. Mag. B 80 (2000) 1757.
[13] I. Petri, P.S. Salmon, H.E. Fischer, Phys. Rev. Lett. 84 (2000) 2413.
[14] P.S. Salmon, I. Petri, J. Phys. Condens. Matter 15 (2003) S1509.
[15] For a recent example of the application to amorphous $GeSe_2$ of interatomic potentials derived from first-principles data see J.C. Mauro, A.K. Varshneya. J. Am. Ceram. Soc. 89 (2006) 2323.
[16] P.S. Salmon, J. Non-Cryst. Solids 353 (2007) 2959.
[17] C. Massobrio, A. Pasquarello, Phys. Rev. B 77 (2008) 144207.
[18] I. Petri, P.S. Salmon, Phys. Chem. Glasses 43C (2002) 185.
[19] R. Car, M. Parrinello, Phys. Rev. Lett. 55 (1985) 2471.
[20] K. Laasonen, A. Pasquarello, R. Car, C. Lee, D. Vanderbilt, Phys. Rev. B 47 (1993) 10142.
[21] C. Massobrio, A. Pasquarello, J. Phys. Condens. Matter 19 (2007) 415111.
[22] J.P. Perdew, Y. Wang, Phys. Rev. B 45 (1992) 13244.
[23] G. Kresse, J. Hafner, Phys. Rev. B 49 (1994) 14251.
[24] R.V. Kulkarni, W.G. Aulbur, D. Stroud, Phys. Rev. B 55 (1997) 6896.
[25] P.S. Salmon, J. Phys. F: Met. Phys. 18 (1988) 2345.
[26] J.P. Gabathuler, S. Steeb, Z. Naturforsch. Teil A 34 (1979) 1314.
[27] A.D. Becke, Phys. Rev. A 38 (1988) 3098.
[28] C. Lee, W. Yang, R.G. Parr, Phys. Rev. B 37 (1988) 785.
[29] R. Colle, O. Salvetti, Theor. Chim. Acta 37 (1975) 329.
[30] S. Nosé, Mol. Phys. 52 (1984) 255;
W.G. Hoover, Phys. Rev. A 31 (1985) 1695.
[31] P.E. Blöchl, M. Parrinello, Phys. Rev. B 45 (1992) 9413.
[32] A.B. Bhatia, D.E. Thornton, Phys. Rev. B 2 (1970) 3004.
[33] P.S. Salmon, Proc. R. Soc. Lond. A 437 (1992) 591.
[34] For the explicit relationship between the three sets of partial structure factors commonly used (Faber-Ziman, Ashcroft-Langreth and Bhatia-Thornton) see H.E. Fischer, A.C. Barnes, P.S. Salmon. Rep. Prog. Phys. 69 (2006) 233.
[35] C. Massobrio, M. Celino, A. Pasquarello, Phys. Rev. B 70 (2004) 174202.